



Effect of oxide ion donors on the corrosion and dechromization of stainless steels in KCl–NaCl–BaCl₂ melt

H.A. Abd EL-RAHMAN*, A. BARAKA and S.A. Abd EL-GWAD
Chemistry Department, Faculty of Science, Cairo University, Giza, Egypt
(* author for correspondence, e-mail: harahman@chem-sci.cairo.eun.eg)

Received 27 October 1997; accepted in revised form 10 February 1998

Key words: corrosion, dechromization, molten chloride, oxyanions, selective leaching, stainless steel

Abstract

The corrosion behaviour of several austenitic and ferritic stainless steels was studied in the KCl–NaCl–BaCl₂ melt (molar ratio 1:1:1) at 600 °C in the absence and presence of 0.1 molal sodium salts with different oxyanions, namely, Na₂CO₃, Na₂O₂, Na₂SO₃, Na₂SO₄, Na₃PO₄ and Na₄P₂O₇. The corrosion rate, determined from analysis of the melt by atomic absorption, was found to agree well with that determined from anodic polarization and decreased with increasing percentage Cr in the alloy. The presence of the oxyanions led to a decrease in the corrosion rate in the order: P₂O₇⁴⁻ < PO₄³⁻ < SO₃²⁻ < SO₄²⁻ < O₂²⁻ < CO₃²⁻ which runs parallel to the order of increasing ability of O²⁻ ion donation and indicates that the inhibition process involves the formation of a passivating film on the surface. All stainless steels were found to suffer a significant selective leaching of chromium and among all the oxyanions tested, only CO₃²⁻ anions suppressed the dechromization in the KCl–NaCl–BaCl₂ melt significantly.

1. Introduction

Chloride melts are of special interest for the electrolytic production of metals like Li [1–3], In [4, 5] and rare earth elements [6, 7] and as quenching media in metallurgical processes [8]. The corrosion of several grades of stainless steel in different chloride melts have been investigated [9–19] and the most serious problem seems to be the dechromization of the alloys in this melt [20]. In the present study, the dechromization of several austenitic and ferritic stainless steels in the KCl–NaCl–BaCl₂ melt (molar ratio 1:1:1) and the role of small additions of sodium salts with oxyanions on suppression of the corrosion and the selective leaching of chromium is studied. The KCl–NaCl–BaCl₂ melt allowed us to conduct corrosion studies on stainless steels at lower temperatures than that possible in binary chloride melts such as KCl–NaCl and KCl–MgCl₂.

2. Experimental details

The electrodes were cut from sheets (about 1 mm thick) of the tested stainless steels with the compositions given in Table 1. The electrodes were 1 cm × 1 cm with a side arm of about 20 cm long and 0.2 cm width, used for electrical connection. Before immersion in the melt, the electrode surface was polished with emery papers down to 4/0 grade and degreased with ether. The KCl–NaCl–

BaCl₂ melt (m.p. 540 °C) was prepared by mixing 1:1:1 (molar ratio) of the anhydrous salts (analytical grades, Merck), melting them at 600 °C for several hours to eliminate traces of water, cooling the melt and storing in dry atmosphere. The electrolytic cell, the electric furnace and the rest of the experimental details were essentially those described elsewhere [21]. The reference electrode was a Ag/AgCl electrode in the KCl–NaCl–BaCl₂ melt in a separate Pyrex glass tube.

The auxiliary electrode consisted of two identical large Pt sheets about 2 cm × 1 cm (each in a Pyrex glass tube with a medium porosity sintered glass disc and was placed at one side of the working electrode. The following analytical grade salts were added to the melt without further treatment: Na₂CO₃, Na₂O₂, Na₂SO₃, Na₂SO₄ and Na₄P₂O₇. Analytical grade Na₃PO₄ 12 H₂O was used after heating at 150 °C for several hours. Before immersing the electrodes in the electrolytic cell, the melt, with or without the additive, was kept at 600 °C for 2 h to ensure the complete dehydration of the melt. A stream of nitrogen gas was allowed to pass over the melt surface during the corrosion experiment.

Atomic absorption spectroscopy (Perkin–Elmer, model 238) was used for the determination of the concentration of Fe, Cr and Ni cations dissolved in the melt after specific corrosion times. In each experiment, three 0.5 g samples from the solidified melt were analyzed and the average values were taken. The thin

Table 1. Composition of the commercial stainless steels used in the study

Alloy	Composition/wt%									Type*
	Fe	C	Si	Mn	Cr	Ni	P	S	Mo	
1	85.88	0.080	0.627	0.357	12.92	0.31	0.004	0.008	0.026	405
2	83.48	0.062	0.439	0.374	15.03	0.35	0.005	0.010	0.044	429
3	72.74	0.064	0.496	1.38	17.90	7.08	0.005	0.000	0.129	301
4	68.90	0.086	0.489	1.53	19.20	9.49	0.015	0.008	0.109	304
5	69.35	0.053	0.511	0.992	20.45	8.37	0.005	0.000	0.072	304

* The type of stainless steel was determined with reference to the standards given by AISI.

corrosion layers remaining on the alloy surfaces were removed carefully using a plastic knife and analysed.

3. Results and discussion

3.1. Corrosion in the pure melt

Two methods were employed to estimate the corrosion of the five stainless steels; a differential method which involved the determination of the main corrosion products, namely, Fe, Cr and Ni ions in the melt or in the scale left after corrosion by atomic absorption and an integral method which involved the determination of the corrosion rate by the anodic polarization characteristics. Figure 1 shows the mass increase of Fe, Cr and Ni in the melt with time of corrosion for the five stainless steels. Except for the initial stage of corrosion at <1 h, the rate of dissolution of either Fe, Cr or Ni from the steel is practically constant over the corrosion period of 6 h. Due to the very low Ni content in the ferritic alloys 1 and 2 (Ni% ~ 0.3%), the Ni analysis for these two alloys was not performed. The corrosion rate, R , was determined from the data given in Fig. 1 by summing the slopes (in $\mu\text{g cm}^{-2} \text{h}^{-1}$) for the Fe, Cr and Ni components. The contribution of the thin corrosion layer on the alloy surface was neglected in the calculation of the corrosion rate. Figure 2 shows the anodic polarization curves (Tafel plots) for the five alloys in the melt after the attainment of the steady corrosion potential, E_{corr} . The corrosion current, i_{corr} , was determined from Tafel plots using the relation: $E - E_{\text{corr}} = a + b \log i$, where b is the Tafel slope and a is the intercept and equals $-b \log i_{\text{corr}}$. Figure 3 shows the dependence of both R and i_{corr} on percentage Cr in the alloy. The quantitative comparison between R and i_{corr} can be made through the application of Faraday's law:

$$R(\mu\text{g cm}^{-2} \text{h}^{-1}) = i_{\text{corr}}(\mu\text{A cm}^{-2}) \times A_w \times 60 \times 60/nF$$

where A_w is the atomic weight of the dissolved element, n is the valence of its cation and F is the Faraday constant. Assuming that $A_w = 55.8$ and $n = 2$ (for Fe), $R = 1.04 i_{\text{corr}}$. The quantitative agreement between the corrosion rates determined by the two methods is clear. Generally, the corrosion rate decreases with increasing percentage Cr, although the increase in percentage Cr from 12% to 20% leads to only a 20–30% decrease in

the corrosion rate. Compared with other chloride melts like the KCl–NaCl eutectic or the KCl–NaCl–MgCl₂ eutectic, the corrosion rate in the KCl–NaCl–BaCl₂ melt is higher [21], most probably due to the traces of water which could not be eliminated by heating the melt for several hours before use.

3.2. Selective leaching of chromium

The data in Fig. 1 were used to estimate the selective leaching factor, f_{SL} , for each of the main alloy components, namely, Fe, Cr and Ni as follows:

$$f_{\text{SL}}^i = \frac{(\text{mass of } i \text{ in the melt}) \times 100}{(\sum_i \text{ mass of } i \text{ in the melt}) \times i\% \text{ in the alloy}}$$

where $i = \text{Fe, Cr or Ni}$. The variation of f_{SL}^i with time for the alloys is shown in Fig. 4. Naturally $f_{\text{SL}}^i < 1$ means surface enrichment with the component, $i f_{\text{SL}}^i > 1$ means the selective leaching of component i and $f_{\text{SL}}^i = 1$ indicates uniform corrosion. Inspection of Fig. 4 indicates selective leaching of Cr from the surface layer for all alloys and surface enrichment with Fe and Ni, as reported previously in other chloride melts [21]. Increasing the percentage Cr in the alloy seems to aid the resistance against dechromization slightly and to a lesser extent the surface enrichment with Ni. The significant loss of Cr from the alloy surface leads to the diffusion of Cr from inside the alloy towards the corroding surface layer to compensate for the depletion of Cr and, consequently, a significant deterioration of the mechanical properties for the surface layer, as well as for the bulk alloy, is expected as a result of corrosion.

The corrosion of the tested alloys in the KCl–NaCl–BaCl₂ melt also leads to the formation of loosely adherent scales on the corroding surfaces. The concentration of Fe, Cr and Ni ion in the scales are much higher than in the melt, as can be seen in Table 2, and the f_{SL} values for Cr are slightly lower than in the melt.

3.3. Effect of addition of oxyanions on corrosion rate

The addition of 0.1 M sodium salts with different oxyanions, namely, Na₂O₂, Na₂CO₃, Na₂SO₄, Na₂SO₄, Na₃PO₄ and Na₄P₂O₇ on both the corrosion rate and the selective leaching of Cr was studied. Figure 5 shows the variation of the steady corrosion potential with

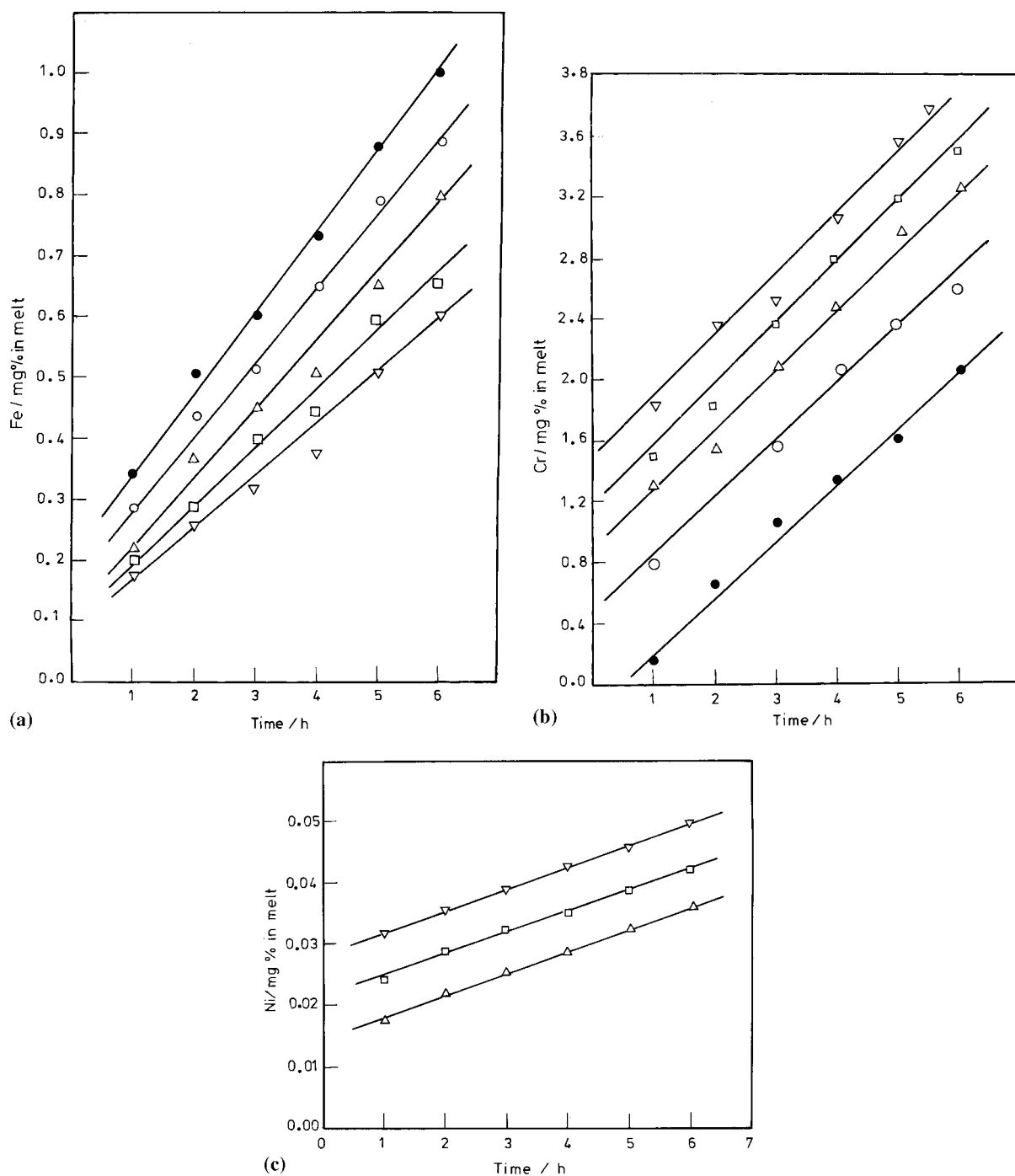


Fig. 1. Mass increase of metal cations in the KCl-NaCl-BaCl₂ melt with time during corrosion of stainless steels: (a) Cr, (b) Fe and (c) Ni. Alloy number: (●) 1, (○) 2, (△) 3, (□) 4 and (▽) 5.

percentage Cr in the presence of the various oxyanions. Generally, E_{corr} shifts to more anodic values as percentage Cr increases, regardless of the additive type. The presence of oxyanions leads to an anodic shift in E_{corr} in the order: pure melt $\sim \text{P}_2\text{O}_7^{4-} < \text{PO}_4^{3-} < \text{SO}_3^{2-} < \text{SO}_4^{2-} < \text{O}_2^{2-} \sim \text{CO}_3^{2-}$. The order runs almost parallel to the order of the basic character of the oxyanion (i.e., the ability to donate O^{2-} ions) [22]. The anodic shift of E_{corr} with either percentage Cr or the basic character of the anion added is accompanied by a decrease in the corrosion current (Table 3) which indicates that the anodic shift in E_{corr} is

attributable to a passivating process which retards the dissolution of the alloy constituents.

Figure 6 is an example of the effect of the oxyanions on the anodic polarization curves of the stainless steels in the KCl-NaCl-BaCl₂ melt at 600 °C. Although the curves in Fig. 6 do not exhibit a definite region of passivity, the tendency to develop passivity increases with increasing basic character of the oxyanion. The i_{corr} values estimated from the curves in Fig. 6 are given in Table 3 and clearly show that the oxyanions act as corrosion inhibitors, where the inhibition efficiency

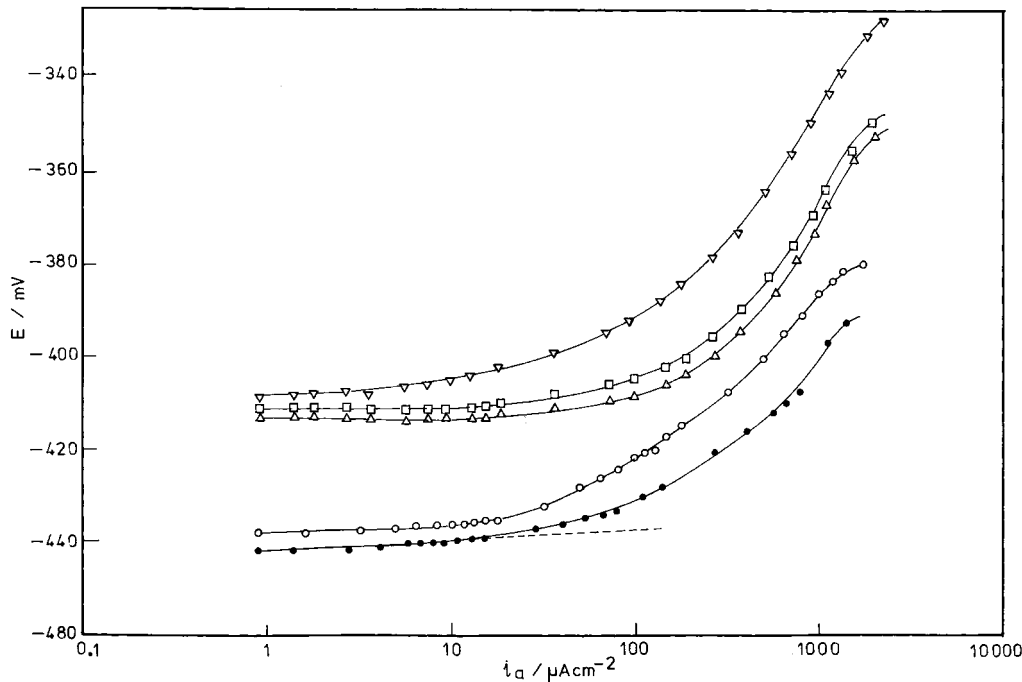


Fig. 2. Anodic polarization curves for stainless steels in the KCl-NaCl-BaCl₂ melt at 600 °C. The dashed line refers to the Tafel region used for the determination of corrosion current. Alloy number: (●) 1, (○) 2, (△) 3, (□) 4 and (▽) 5.

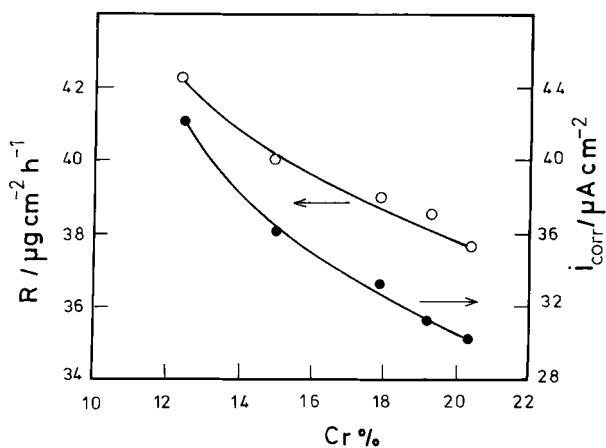


Fig. 3. Dependence of the corrosion rate, R , and the corrosion current, i_{corr} , on the percentage Cr.

Table 2. Concentration of the metal cations* in the scale on alloys after corrosion for 4 h in the KCl-NaCl-BaCl₂ melt at 600 °C

Alloy	Concentration of cation/mg% (f_{SL})		
	Fe	Cr	Ni
1	12.46 (0.51)	15.82 (4.50)	—
2	11.05 (0.49)	16.15 (3.95)	—
3	8.49 (0.41)	19.59 (3.82)	0.21 (0.11)
4	7.06 (0.35)	21.85 (3.89)	0.33 (0.12)
5	7.63 (0.35)	23.82 (3.67)	0.27 (0.10)

*The values between parentheses refer to the selective leaching factors, f_{SL} .

increases generally as the basic character increases: pure melt < Na₃PO₄ < Na₂SO₄ ~ Na₂SO₃ < Na₂O₂ < Na₂CO₃. The corrosion inhibition of the stainless steels

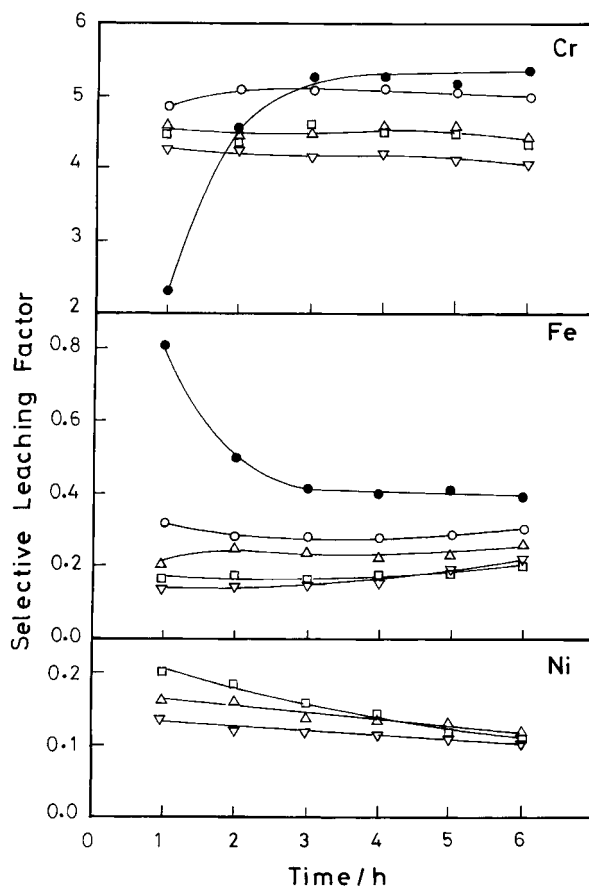


Fig. 4. Variation of the selective leaching factor for Cr, Fe and Ni with time for the stainless steels in the KCl-NaCl-BaCl₂ melt at 600 °C. Alloy number: (●) 1, (○) 2, (△) 3, (□) 4 and (▽) 5.

in the presence of O²⁻ ion donors is due to the formation of a passivating oxide layer on the alloy surface which

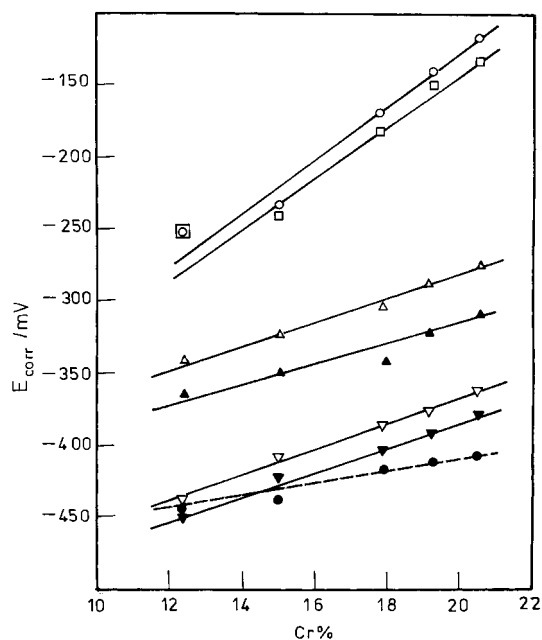


Fig. 5. Dependence of the steady corrosion potential, E_{corr} , on percentage Cr in the stainless steel in the KCl–NaCl–BaCl₂ melt containing 0.1 M of sodium salts with different oxyanions: (○) Na₂CO₃, (□) Na₂O₂, (△) Na₂SO₄, (▲) Na₂SO₃, (▽) Na₃PO₄ and (▼) Na₄P₂O₇. The dashed line refers to the pure melt. Temperature 600 °C.

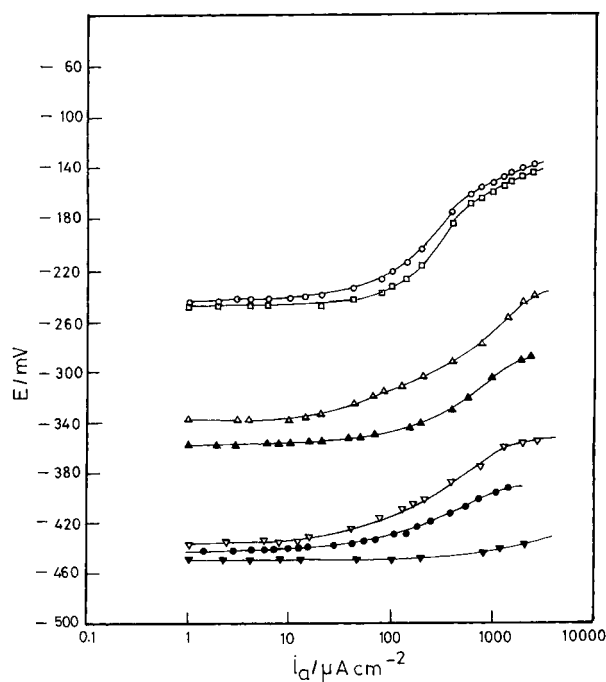


Fig. 6. Anodic polarization curves for the alloy 1 in the KCl–NaCl–BaCl₂ melt containing 0.1 M of sodium salts with different oxyanions: (○) Na₂CO₃, (□) Na₂O₂, (△) Na₂SO₄, (▲) Na₂SO₃, (▽) Na₃PO₄ and (▼) Na₄P₂O₇. Temperature 600 °C.

Table 3. Corrosion current and inhibition percent* for stainless steels in the KCl–NaCl–BaCl₂ melt containing 0.1 molal of sodium salts of different oxyanions at 600 °C

Alloy	Pure melt	Na ₂ CO ₃	Na ₂ O ₂	Na ₂ SO ₄	Na ₂ SO ₃	Na ₃ PO ₄
1	42	18 (57)	22 (48)	26 (38)	32 (23)	34 (19)
2	36	14 (61)	15 (58)	18 (50)	22 (39)	30 (29)
3	33	14 (58)	12 (64)	19 (42)	13 (61)	23 (30)
4	32	9 (17)	10 (68)	20 (37)	18 (43)	26 (17)
5	30	13 (57)	14 (53)	16 (47)	14 (53)	25 (17)

*The i_{corr} values are given in $\mu\text{A cm}^{-2}$ and the values between parentheses refer to the inhibition percent, $I\% = \{1 - [(i_{\text{corr}})_{\text{with additive}} / (i_{\text{corr}})_{\text{pure melt}}]\} \times 100$.

Table 4. Selective leaching factors for alloy 3 in the KCl–NaCl–BaCl₂ melt at 600 °C in the presence of 0.1 molal of sodium salts of different oxyanions after corrosion, for 4 h

Addition	Selective leaching factor, f_{SL}		
	Fe	Cr	Ni
Pure	0.23	4.62	0.12
Na ₂ CO ₃	0.96	1.57	0.31
Na ₂ O ₂	0.66	2.78	0.35
Na ₂ SO ₄	0.35	4.08	0.21
Na ₂ SO ₃	0.23	4.59	0.13
Na ₃ PO ₄	0.23	4.60	0.13
Na ₄ P ₂ O ₇	0.23	4.61	0.13

acts as a physical barrier against dissolution of the alloy components into the melt in the form of soluble cations.

3.4. Effect of addition of oxyanions on the dechromization

To study the effect of addition of oxyanions on the selective leaching of Cr, one of the five stainless steels (alloy 3) was immersed in the KCl–NaCl–BaCl₂ melt in

the presence of 0.1 M of various oxyanions at 600 °C for 4 h. Samples of the melt, after corrosion, were quantitatively analysed by atomic absorption spectrophotometry for Fe, Cr and Ni and the results are given in Table 4. It is most interesting to see that only CO₃²⁻ anions (and to lesser extent O₂²⁻ anions) lead to a significant improvement in the f_{SL} values towards the prevention of such a form of corrosion. The rest of the oxyanions have no significant effect on the selective leaching of percentage Cr. Thus addition of Na₂CO₃ can lead to significant suppression of both the corrosion rate and the selective leaching of Cr from the stainless steel in KCl–NaCl–BaCl₂ melt.

4. Conclusion

Austenitic and ferritic stainless steels with 12–20% Cr suffer corrosion with significant selective leaching of chromium in the KCl–NaCl–BaCl₂ melt at 600 °C. Small additions of sodium salts with O²⁻ ion donating ability leads to 17–71% suppression of corrosion with

Na₂CO₃ having the greatest effect in suppression of both corrosion and dechromization.

References

1. W.E. Cowley, *The alkali metals in 'Molten Salt Technology'* (edited by D. G. Lovering), Plenum Press, New York (1978), p. 57.
2. W.A. Averill and D.L. Olson, *Energy* **3** (1978) 305.
3. W.H. Kruesi and D.J. Fray, *J. Appl. Electrochem.* **24** (1994) 1102.
4. B.N. Popov and J. Vivshin, *Croatica Chem. Acta* **60** (1987) 315.
5. J. Bouteillon, M. Jafarian, J.C. Poignet and A. Reydet, *J. Electrochem. Soc.* **139** (1992) 1.
6. G. Xie, K. Ema, Y. Ito and M.S. Zhao, *J. Appl. Electrochem.* **23** (1993) 753.
7. Y. Katayama, R. Hagiwara and Y. Ito, *J. Electrochem. Soc.* **142** (1995) 2174.
8. Y. Lakhtin, *'Engineering Physical Metallurgy'*, Mir Publisher, Moscow (1971), chapter 9, p. 197.
9. S.I. Stepanov, *Zashch. Met.* **7** (1971) 35.
10. I.N. Ozeryanaya, N.A. Krasil'nikov, S.M. Perin, M.V. Smirnov and N.D. Shamanova, *Zashch. Met.* **14** (1978) 321.
11. D.O. Raleigh, J.T. White and C.A. Ogden, *J. Electrochem. Soc.* **12** (1979) 1093.
12. O.V. Mazova, V.P. Volodin, S.M. Beloglazov, *Zashch. Met.* **17** (1981) 216.
13. P.F. Tortorelli, J.H. Devon and J.R. Keiser, *J. Nucl. Mater.* **103** (1981) 675.
14. D.F. Heine, *Heat Recovery Syst. CHP* **7** (1987) 389.
15. M. Balbi, G. Tosi, A. LaVecchia and A. Barbangelo, *Acciaio Inossid* **45** (1978) 12.
16. H. Atmani and J.J. Rameau, *Corros. Sci.* **24** (1984) 279.
17. H. Atmani and J.J. Rameau, *Mater. Sci. Eng.* **88** (1987) 221.
18. H. Atmani and J.J. Rameau, *Mater. Sci. Eng.* **88** (1987) 247.
19. H. Atmani and J.J. Rameau, *Corros. Sci.* **27** (1987) 35.
20. H.A. Abd El-Rahman, A.M. Baraka, M.S. Morsi and S.A. Abd El-Gwad, *Thin Solid Films* **247** (1994) 56.
21. A.M. Shams El-Din and A.A. Gergers, in *'Electrochemistry'* (edited by H. Friend and F. Gutman), Pergamon, New York (1964), p. 62.